2016 IEEE International Conference on Advanced Intelligent Mechatronics (AIM)
Banff, Alberta, Canada, July 12–15, 2016

Bilateral Shared Autonomous System for MUMAV with Nonpassive Human and Environment Input Interaction Forces

Shafiqul Islam, Jorge Dias, Lakmal D. Seneviratne

Abstract— **In this paper, the stability and synchronization control problem of bilateral shared autonomous system for miniature unmanned multirotor aerial vehicle (MUMAV) is addressed with nonpassive human and environment input forces. The master input interface design combines scaled position of the master manipulator with velocity signals of the MUMAV and reflected remote interaction forces. The slave input interaction interface is designed by combining scaled position and velocity of the master manipulator with the velocity of the remote slave MUMAV system. The data transmission between local master and remote MUMAV is assumed to be carried out by using dedicated internet communication network with negligible time delay. The convergence analysis is shown by using Lyapunov method. The analysis shows that the closed loop bilateral shared autonomous system is input-to-state stable and ultimately bounded with nonpassive human and environment input interaction force.**

I. Introduction

One of the main challenges in robotics is to operate the robot and perform tasks autonomously in unstructured unknown environments. In fact, autonomous robotic systems are limited in their applications as they need to use assumptions about the operating environments. Therefore, it is very difficult for autonomous robotic system to perform tasks such as remote manipulations, inspection, surveillance, search and rescue task precisely and safely as they demands highly trained human operator. On the other hand, human operator is highly trained and can perform above mentioned tasks precisely and safely. So, human operator can be integrated into the loop so as to perform remote operation and manipulation task precisely and safely. However, an experienced operator may lack the situational awareness about the surrounding environment of the robot to perform remote operation and manipulation tasks. Therefore, it is very important to integrate haptic interface between local and remote platform in order to achieve navigation, control, tracking, and inspection and interaction/manipulation tasks precisely and safely in uncertain remote environment.

Initial research in the field of remotely operated MUMAV utilized mainly vision feedback by either keeping the vehicle in line of sight of the operator or using images coming from on board vision system [1, 2, 3]. These designs do not use haptic sensor to map the surrounding environment for maneuvering the vehicle. Also, the limited resolution and field of view of on board cameras, high dependence on weather conditions and high transmission latency of image data results in reduced situational awareness. In [4, 5], authors proposed artificial force fields technique from mobile robotic research [11] to map the environment force to the operators hand through haptic feedback so that operator can avoid obstacle by increasing situational awareness about the surrounding environment of MUMAV. Authors in [6] used optical flow from on board camera to generate force feedback to guide the human operator for avoiding collisions of the remotely operated flying vehicle. Authors in [7, 10, 18, 19] developed remotely operated shared navigation system for MUMAV for indoor environments by combining a vision based obstacle-avoidance technique with haptic feedback. In [20], [21] authors presented a shared autonomous system for MUMAV for indoor environments using with visual and haptic feedback. Authors in [22-24] proposed control strategy for remote operation for MUMAV. Most reported designs mainly focused on avoiding surrounding environments of the flying vehicle by assuming that the environment can be mapped with the help of vision and/or laser technology to the operator hand via haptic device. Also, most existing designs do not consider synchronization of the movement between master and MUMAV system. Moreover, the existing interaction interface does not allow MUMAV to directly or indirectly interact with nonpassive environment.

In this work, we develop coordination control interface for bilateral shared autonomous system for MUMAV for direct interaction with environment. The proposed interface allows operator to navigate, control and synchronize motion between slave MUMAV and master manipulator in the presence of nonpassive human and environment input interaction forces. The shared coordination control interface for master manipulator is designed by combining velocity states of the slave MUMAV with the scaled position of the master manipulator. The reflected force from the interaction between nonpassive environment and slave MUMAV is also integrated with the master input interface that allows the operator to directly perceive the information about the interaction environment of the MUMAV. The shared control for the slave is developed by combining scaled position and velocity of the master manipulator with the velocity of the remote MUMAV. The stability analysis is shown by using Lyapunov method provided that the data transmission delays between local and remote platform are negligible. It is shown in our analysis that all the states are input-to-state stable and ultimately bounded under nonpassive interaction between MUMAV and environment and between master and human operator.

S. Islam is with University Ottawa, Ottawa, Canada, and Khalifa University, 127788 Abu Dhabi, UAE.

J. Dias is with University of Coimbra, Portugal and KUSTAR, Abu Dhabi, 1027788 UAE.

L. D. Seneviratne is with Kings College Londdon, UK, and Khalifa University, 127788 Abu Dhabi, UAE.

978-1-5090-2065-2/16/$31.00 ©2016 IEEE

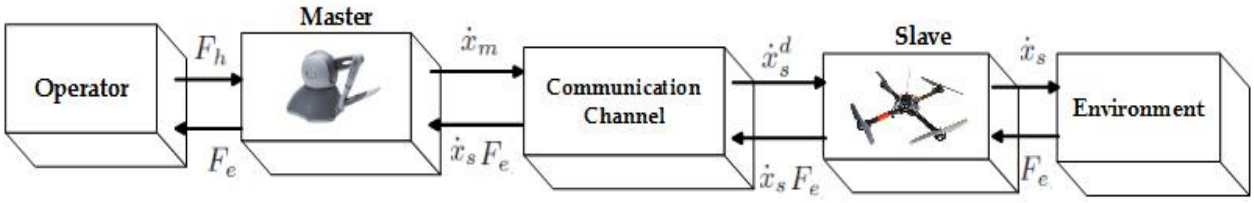

Fig. 1. Block diagram representation of the bilateral shared autonomous system for MUMAV.

This paper is organized as follows: In section II, dynamical model and coordination control interface for bilateral shared autonomous system for MUMAV is presented. Section II also presents detail convergence analysis. Section III concludes the paper.

II. Modeling, Bilateral Shared Control Interface Algorithm and Convergence Analysis

In this section, we first develop model for designing haptic based bilateral shared control input interface strategy for MUMAV. Block diagram representation of the bilateral shared autonomous system is depicted in Fig. 1. Fig. shows the data flow diagram describing the overall system components that consists of a master manipulator, a slave manipulator, a communication network, a human operator, interaction model between master and slave as well as a remote environment.

Let us first model ground master system interacting with human operator. The motion dynamic for the 3-DOF master haptic manipulator interacting with human operator can be written in Cartesian state space form as follows [13]

$$M_m \ddot{x}_m + B_m \dot{x}_m = f_m + f_h \tag{1}$$

where $\ddot{x}_m$, $\dot{x}_m$ and x_m are the acceleration, velocity and position of the haptic manipulator, M_m is the diagonal symmetric positive definite inertia matrix, B_m is the diagonal matrix of damping coefficient, f_m is the control force vector and f_h is the force vector applied to the haptic manipulator by the human operator expressed in fixed inertial frame $\mathcal{I}$. In our design, a human operator commands the desired velocity for MUMAV in fixed inertial frame $\mathcal{I}$. Now, using x_{m1}, x_{m2} and x_{m3}, the desired velocities are mapped on the MUMAV as x_{s1}, x_{s2} and x_{s3} as follows

$$\dot{x}_s^d = k_v x_m \tag{2}$$

with a constant scaling diagonal matrices $k_v \in \Re^{3\times 3}$, $x_m = [x_{m1}\, x_{m2}\, x_{m3}]^T$ and $\dot{x}_s^d = [\dot{x}_{s1}^d\, \dot{x}_{s2}^d\, \dot{x}_{s3}^d]^T$. The shared control input interaction interface for master system combines velocity signals of the remote slave with the scaled position of the master haptic manipulator and reflected interaction force between remote environment and MUMAV. Then, the shared coordination control interface for master can be designed as follows

$$f_m = K_{ph}\left(\dot{x}_s - \alpha_s x_m\right) - K_{dh}\dot{x}_m - f_e \tag{3}$$

where $K_{ph} \in \Re^{3\times 3}$ and $K_{dh} \in \Re^{3\times 3}$ are the symmetric positive definite constant matrices and the scaling factor α_s. The bounds on α_s is chosen according to the boundaries of the master as calculated as $\alpha_s = \frac{(max(x_s)-min(x_s))}{(max(x_m)-min(x_m))}$. The term f_e is the reflected interaction force between remote environment and slave to the human operator. The interaction force f_h and f_e is assumed to be available by either direct measurement or estimation technique.

We now derive the dynamical model the quadrotor UAV as a slave system. Using Euler-Newton formula, the motion dynamic of 6-DOF underactuated slave quadrotor UAV system can be written by the following equation [14]-[16]

$$J_s\dot{\Omega}_s = f_{sa} - S(\Omega_s)J_s\Omega_s \tag{4}$$
$$m_s\ddot{x}_s = -f_{st}R_s\mathcal{I}_3 + m_s g\mathcal{I}_3 \tag{5}$$

where m_s defines the mass, g represents gravity constant, $x_s = [x_{s1}, x_{s2}, x_{s3}]^T$ denotes the position with respect to fixed inertial frame $\mathcal{I}$, $\Omega_s = [\Omega_{s1}, \Omega_{s2}, \Omega_{s3}]^T$ expressed the angular velocity of the vehicle in body frame $\mathcal{B}_u$, J_s defines the inertia matrix in $\mathcal{B}_u$, R_s represents the rotational matrix representing the vehicles body frame $\mathcal{B}_u$ with respect to $\mathcal{I}$, f_{st} denotes thrust control, f_{sa} defines attitude control torques, $S(\Omega_s)$ represents the skew-symmetric operator associated with the cross product $\times$.

Let us now design coordination control input interface algorithm for the system (4) and (5) by using inner-loop attitude and outer-loop translational dynamic configuration. It is assumed in our design that the attitude dynamic (4) is faster than the translational dynamics (5). The control input interface for translational dynamic is designed to ensure $\dot{x}_s$ tracks the desired velocity signals $\dot{x}_s^d$. The same control interface also generates desired rolling and pitching command trajectory for attitude controller. Before developing coordination control interface, let us first define new coordinate for rotational dynamic as $\eta = [\phi\ \theta\ \psi]^T$ with three Euler angles roll, pitch and yaw. Then, the dynamics (4) and (5) can be re-written with respect to new coordinate η as

$$J_s\dot{\Omega}_s = f_{sa} - S(\Omega_s)J_s\Omega_s \tag{6}$$
$$\dot{\eta} = \mathcal{A}(\eta)\Omega_s \tag{7}$$
$$m_s\ddot{x}_s = -f_{st}R_s(\eta)\mathcal{I}_3 + m_s g\mathcal{I}_3 \tag{8}$$

with the transformation matrix $\mathcal{A} \in \Re^{3\times 3}$ and $R_s(\eta) \in \Re^{3\times 3}$. Then, the dynamical model for translational subsystems (8) for the first, second and third row can be re-defined

as follows

$$m\ddot{x}_{s1} = -f_{st}\sin\phi\sin\psi - f_{st}\cos\phi\cos\psi\sin\theta \quad (9)$$
$$m\ddot{x}_{s2} = -f_{st}\cos\phi\sin\theta\sin\psi + f_{st}\sin\phi\cos\psi \quad (10)$$
$$m\ddot{x}_{s3} = -f_{st}\cos\theta\cos\phi + mg \quad (11)$$

where $\ddot{x}_{s1}$, $\ddot{x}_{s2}$, $\ddot{x}_{s3}$ are the linear acceleration, $\dot{x}_{s1}$, $\dot{x}_{s2}$, $\dot{x}_{s3}$ are the linear velocity, x_{s2}, x_{s2}, x_{s3} are the linear position. f_{st} is the thrust vector and $f_{sa} = [f_{s\phi}\ f_{s\theta}\ f_{s\psi}]^T$ is the attitude control input torque.

We first design controller for attitude dynamics (6) and (7). To do that, we define desired coordinate $\eta_d = [\phi_d\ \theta_d\ \Psi_d]^T$. The desired attitude commands ϕ_d and θ_d is provided by the output of the outer-loop control f_{sx} and f_{sy} (16). Then, the error model for attitude dynamics can be written as

$$\ddot{e}_\eta = \mathcal{A}(\eta)J_s^{-1}S(\Omega_s)J_s\Omega_s - \mathcal{A}(\eta)J_s^{-1}f_{sa} - \dot{\mathcal{A}}_\eta \mathcal{A}^{-1}(\eta)\dot{\eta} + \ddot{\eta}_d \quad (12)$$

For our design, we consider that the attitude angles are bounded as $-\frac{\pi}{2} < \phi < \frac{\pi}{2}$, $-\frac{\pi}{2} < \theta < \frac{\pi}{2}$ and $-\pi < \psi < \pi$. Since the angles ϕ, θ and ψ are bounded, then we can also assume that the matrices $\mathcal{A}^{-1}(\eta)$ are bounded as $\|\mathcal{A}^{-1}(\eta)\| \leq \delta_L$ with $\delta_L > 0$. Then, the input torque f_{sa} is designed as follows

$$f_{sa} = \mathcal{A}^{-1}(\eta)J_s\left(K_p(\eta_d - \eta) + K_d(\dot{\eta}_d - \dot{\eta}) + \ddot{\eta}_d\right) \quad (13)$$

where K_p and K_d are the constant diagonal matrices. The horizontal motion can be achieved by rolling and pitching the vehicle for the given reference signals $\dot{x}_s^d$ provided by master manipulator. The desired yaw is provided by designer. So, the vectors f_{sx} and f_{sy} are the control to drive the translational dynamics in x_{s1} and x_{s2} to generate the desired rolling and pitching command trajectories ϕ_d and θ_d in (13). To develop controller for f_{sx} and f_{sy}, let us simplify the translational dynamics (9) and (10) as follows

$$m\begin{pmatrix}\ddot{x}_{s1}\\ \ddot{x}_{s2}\end{pmatrix} = -\mathcal{T}_s(\phi,\psi)f_{sz}\begin{pmatrix}\sin\theta\\ \sin\psi\end{pmatrix} \quad (14)$$

with

$$\mathcal{T}_s(\phi,\psi) = \begin{bmatrix}\cos\phi\cos\psi & \sin\psi\\ \cos\phi\sin\psi & -\cos\psi\end{bmatrix}$$

The thruster input vector f_{st} is calculated by the following equation

$$f_{st} = -\frac{m}{\cos\theta\cos\phi}(-g + \ddot{x}_{s3}^d + k_{ds3}(\dot{x}_{s3}^d - \dot{x}_{s3}) + k_{d3}\dot{x}_{s3}) \quad (15)$$

The bounds on f_{st} exists as $\cos\phi \neq \cos\theta \neq 0$. Then, a bilateral shared coordination input for the slave MUMAV can be designed by coupling scaled position and velocity of the master manipulator with the velocity of the MUMAV. The desired rolling and pitching dynamics for attitude controller (13) can be designed as follows

$$f_s = \gamma_p\begin{pmatrix}\ddot{x}_{s1}^d + k_{ds1}\left(\dot{x}_{s1}^d - \dot{x}_{s1}\right) + k_{d1}\dot{x}_{s1}\\ \ddot{x}_{s2}^d + k_{ds2}\left(\dot{x}_{s2}^d - \dot{x}_{s2}\right) + k_{d2}\dot{x}_{s2}\end{pmatrix} \quad (16)$$

where $f_s = [f_{sx}, f_{sy}]^T$, $f_{sx} = \sin\theta_d$, $f_{sy} = \sin\phi_d$, $k_{ds1} > 0$, $k_{ds2} > 0$, $k_{d1} > 0$, $k_{d2} > 0$, $\gamma_p = \frac{m|\mathcal{A}|}{f_{sz}}$ and $\mathcal{A} = \mathcal{T}_s^{-1}$. Note that the inverse of $\mathcal{T}_s$ exists as $\cos\phi \neq 0$. Notice also from (16) that we can tune the gain parameters k_{d1}, k_{d2}, k_{ds1} and k_{ds2} to achieve desired dynamical behavior of θ_d and ϕ_d for the attitude dynamics.

We now consider that the input interaction force between master and human operator and between the slave and remote environments is assumed to be nonpassive as $|f_h| \leq \gamma_h$ and $|f_e| \leq \gamma_e$ with $\gamma_h > 0$ and $\gamma_e > 0$. For the convergence analysis of the closed loop system under nonpassive input interaction forces, we choose the following candidate Lyapunov function

$$V_T = V_m + V_s \quad (17)$$

with

$$V_m = \frac{1}{2}\dot{x}_m^T M_m\dot{x}_m + \frac{\alpha_p}{2}x_m^T x_m$$
$$V_s = \frac{1}{2}\dot{\tilde{\eta}}^T\dot{\tilde{\eta}} + \frac{1}{2}\dot{\tilde{\xi}}^T\dot{\tilde{\xi}} \quad (18)$$

with $\alpha_p = \alpha_s\lambda_{min}(K_{ph})$, $\tilde{\eta} = (\eta_d - \eta)$ and $\tilde{\xi} = (x_s^d - x_s)$. The time derivative of $\dot{V}_m$ can be written as follows

$$\dot{V}_m \leq -\dot{x}_m^T\Lambda\dot{x}_m + \dot{x}_m^T\tilde{f}_{he} + \dot{x}_m^T K_{ph}\dot{x}_s \quad (19)$$

with $\Lambda = (B_m + K_{dh})$, $\alpha_p = \lambda_{min}(K_{ph})\,\alpha_s$ and $\tilde{f}_{he} = (f_h - f_e)$. Applying $2a^Tb \leq \delta_1 a^Ta + \frac{1}{\delta_1}b^Tb$ with $\delta_1 > 0$, we can write the following inequality for the last two terms

$$\dot{x}_m^T\tilde{f}_{he} \leq \frac{\lambda_{min}(\Lambda)\|\dot{x}_m\|^2}{2} + \frac{\|\tilde{f}_{he}\|^2}{2\lambda_{min}(\Lambda)}$$
$$\dot{x}_m^T K_{ph}\dot{x}_s \leq \frac{\lambda_{max}^2(K_{ph})\|\dot{x}_s\|^2}{2\lambda_{min(\mathcal{K}_2)}} + \frac{\|\dot{x}_m\|^2}{2\lambda_{min}(\mathcal{K}_2)} \quad (20)$$

Using (20), $\dot{V}_m$ can be written as

$$\dot{V}_m \leq -\lambda_{min}(\Lambda)\|\dot{x}_m\|^2 + \frac{\lambda_{min}(\Lambda)\|\dot{x}_m\|^2}{2} + \frac{\|\tilde{f}_{he}\|^2}{2\lambda_{min}(\Lambda)} + \frac{\lambda_{max}^2(K_{ph})\|\dot{x}_s\|^2}{2\lambda_{min(\mathcal{K}_2)}} + \frac{\|\dot{x}_m\|^2}{2\lambda_{min}(\mathcal{K}_2)} \quad (21)$$

with

$$\mathcal{K}_2 = \begin{bmatrix}k_{d1}\gamma_p & 0 & 0\\ 0 & k_{d2}\gamma_p & 0\\ 0 & 0 & \zeta k_{d3}\end{bmatrix}$$

Now, applying (21), $\dot{V}_T$ can be written as

$$\dot{V}_T \leq -\lambda_{min}(\Lambda)\|\dot{x}_m\|^2 + \frac{\lambda_{min}(\Lambda)\|\dot{x}_m\|^2}{2} + \frac{\|\tilde{f}_{he}\|^2}{2\lambda_{min}(\Lambda)} + \frac{\lambda_{max}^2(K_{ph})\|\dot{x}_s\|^2}{2\lambda_{min(\mathcal{K}_2)}} + \frac{1}{2\lambda_{min}(\mathcal{K}_2)}\|\dot{x}_m\|^2 - \lambda_{min}(\mathcal{K}_2)\|\dot{x}_s\|^2 - \lambda_{min}(\mathcal{K}_o)\|\delta_o\|^2 - \lambda_{min}(\mathcal{K}_1)\|\dot{\tilde{\xi}}\|^2 \quad (22)$$

with

$$\mathcal{K}_o = \begin{bmatrix}\vartheta_a K_P & 0\\ 0 & \vartheta_a K_d\end{bmatrix}, \vartheta_a = \delta_L\upsilon, \|J_s\| \leq \upsilon,$$

$$\mathcal{K}_1 = \begin{bmatrix} k_{ds1}\gamma_p & 0 & 0 \\ 0 & k_{ds2}\gamma_p & 0 \\ 0 & 0 & \zeta k_{ds3} \end{bmatrix}, \zeta = \| \frac{m}{\cos\theta \cos\phi} \|,$$

$\delta_o = [\tilde{\eta}\ \dot{\tilde{\eta}}]^T$. Then, $\dot{V}_T$ can be simplified as

$$\dot{V}_T \leq -\mathcal{B}\|\dot{x}_m\|^2 - \mathcal{C}\|\dot{x}_s\|^2 + \frac{\|\tilde{f}_{he}\|^2}{2\lambda_{min}(\Lambda)} \quad (23)$$

with $\mathcal{B} = \left(\frac{\lambda_{min}(\Lambda)}{2} - \frac{\lambda_{min}(\mathcal{K}_2)}{2}\right)$ and $\mathcal{C} = \left(\lambda_{min}(\mathcal{K}_2) - \frac{\lambda^2_{max}(K_{ph})}{2\lambda_{min(\mathcal{K}_2)}}\right)$. Equation (23) can be further simplified as follows

$$\dot{V}_T \leq -\mathcal{D}\|\Pi\|^2 + \frac{\|\tilde{f}_{he}\|^2}{2\lambda_{min}(\Lambda)} \quad (24)$$

with

$$\mathcal{D} = \begin{bmatrix} \mathcal{B} & 0 & 0 & 0 \\ 0 & \mathcal{C} & 0 & 0 \\ 0 & 0 & \lambda_{min}(\mathcal{K}_o) & 0 \\ 0 & 0 & 0 & \lambda_{min}(\mathcal{K}_1) \end{bmatrix}$$

and $\Pi = [\dot{x}_m\ \dot{x}_s\ \delta_o\ \dot{\tilde{\xi}}]^T$. Since the input interaction forces f_h and f_e are bounded, then the last term of equation (24) is also bounded. Then, $\dot{V}_T$ can be re-written in the following compact form

$$\dot{V}_T \leq -\mathcal{D}\|\Pi\|^2 + \epsilon_o \quad (25)$$

with $\epsilon_o = \frac{\|\tilde{f}_{he}\|^2}{2\lambda_{min}(\Lambda)}$. In view of (25) together with Lyapunov arguments and Barbalat's Lemma, we can conclude that the bilateral shared closed loop system is input-to-state stable with respect to the bounded input interaction forces f_h and f_e, and the states $(x_m, \dot{x}_s, \dot{\tilde{\xi}})$ are ultimately bounded. If the bounds on the input interaction forces f_h and f_e converges to zero, then the bounds of the states $(x_m, \dot{x}_s, \dot{\tilde{\xi}})$ also converges to zero. Based on our above analysis, we can state the following results.

Theorem 1: *Consider the closed loop bilateral shared autonomous system formulated by (1)-(3), (6), (7), (9)-(11), (13), (15), (16) with bounded input interaction forces γ_h and γ_e. Then, if $|f_{st}| > 0$ and the signals $\dot{x}^d_s$ and its first and second derivatives are bounded, then the closed loop system is input-to-state stable with respect to the bounded input interaction force and the states $(x_m, \dot{x}_m, \dot{\tilde{\xi}})$ are ultimately bounded.*

III. Conclusion and Future works

In this paper, the control stability and synchronization problem of bilateral shared autonomous system has been addressed in the presence of nonpassive input interaction with human and environment. The input interface for master has comprised scaled position of the master manipulator with velocity signals of the MUMAV and reflected remote interaction forces between MUMAV and environment. The input interaction interface for slave has developed by combining scaled position and velocity of the master manipulator with the velocity of the remote MUMAV. The design has assumed that the data transmission between local and remote platforms is carried out by dedicated network ensuring negligible data transmission delay. The stability analysis has been shown by using Lyapunov function. The analysis showed the input-to-state stability of the closed loop bilateral shared autonomous system under nonpassive interaction with human and uncertain environment. Unlike other designs, the proposed designed can be used to stabilize and synchronize master manipulator with slave MUMAV under nonpassive human and environment input force. The experimental evaluation of the proposed design on quadrotor UAV system [17] will be part of our future works.

References

[1] M Bernard, J. Andersh, N. Papanikolopoulos, A first investigation into the teleoperation of a miniature rotorcraft, *Experimental Robotics*, Springer, pp. 191-199, 2009.

[2] A. Jonathan, M. Bernard, N. Papanikolopoulos, Experimental investigation of teleoperation performance for miniature rotorcraft, *Proceedings of the 48th IEEE Conference on Decision and Control and Chinese Control Conference*, pp. 6005-6010, 2009.

[3] H. Christoph, M. Jean-Claude, N. Andreas, H. Florian, M. Adrian, B. Christian, B. Samir, S. Dario and S. Roland, Teleoperation assistance for an indoor quadrotor helicopter, *International Conference on Simulation, Modeling and Programming for Autonomous Robots*, Venice, Italy, November 3-4, pp. 464-471, 2008.

[4] L. T. Mung, B. H. Wigert, M. Max, V. P. M. Maria, Artificial force field for haptic feedback in UAV teleoperation, *IEEE Transactions on Systems, Man and Cybernetics, Part A: Systems and Humans*, vol. 39, no. 6, pp. 1316-1230, 2009.

[5] L. T. Mung, B. H. Wigert, M. Max, V. P. M. Maria, Collision avoidance in UAV tele-operation with time delay, *IEEE Proc. on Systems, Man and Cybernetics*, pp. 997-1002, 2007.

[6] M. Robert, S. Felix, C. Peter, O. Y. Siang, A new framework for force feedback teleoperation of robotic vehicles based on optical flow, *IEEE Proc. on Robotics and Automation*, pp.1079-1085, 2009.

[7] C. Raffaella, L. Vincenzo, D. Massimo, F. Matteo, M. Y. Abeje, S. Stefano, B. Siciliano, Robot Vision, *IEEE Robotics and Automation Magazine*, pp. 22, 2013.

[8] R. Andreas, M. Y. Abeje, S. Stefano, C. Raffaella, Kinetic scrolling-based position mapping for haptic teleoperation of unmanned aerial vehicles, *IEEE International Conference on Robotics and Automation*, pp. 3116-3121, 2012.

[9] S. Paolo, B. Massimo, H. H. Blthoff, F, Antonio, A Semi-autonomous UAV Platform for Indoor Remote Operation with Visual and Haptic Feedback, *IEEE International Conference on Robotics and Automation*, Hong Kong, China, 2014.

[10] S. Paolo, B. Massimo, H. H. Blthoff, F. Antonio, Vision-based Autonomous Control of a Quadrotor UAV using an Onboard RGB-D Camera and its Application to Haptic Teleoperation, *2nd IFAC Work. on Research, Education and Development of Unmanned Aerial Systems*, Compiegne, France, 2013.

[11] K. Oussama, Real-time obstacle avoidance for manipulators and mobile robots, *The international journal of robotics research*, vol. 5, no. 1, pp. 90-98, 1986.

[12] K. H. Bruce, A generalized potential field approach to obstacle avoidance control, *Robotics International of SME*, Dearborn, Michigan, USA, RI/SME, 1984.

[13] S. Islam, P. X. Liu and A. El Saddik, Teleoperation systems with symmetrical and unsymmetrical time varying communication delay, *IEEE Transactions on Instrumentation and Measurement*, vol. 62, no. 11, pp. 2943-2953, 2013.

[14] S. Islam, P. X. Liu, A. El Saddik, Nonlinear adaptive control of quadrotor flying vehicle, *Journal of nonlinear Dynamics*, vol. 76, no. 4, pp. 117-133, 2013.

[15] S. Islam, M. Shiekh, R. K. Ashour, J. Dias and L. D. Seneviratne, Robust control of quadrotor UAV, *IEEE ICRA*, May 26-30, Seattle, Washington, USA, 2015, to appear.

[16] S. Islam, L. D. Seneviratne and J. Dias, Adaptive tracking control of quadrotor robot vehicle, *In Proc. IEEE/ASME International Conference on Advanced Intelligent Mechatronics*, July8-11, Besanon, France, pp. 441-445, 2014.

[17] Ascending technologies (AscTec) [Online]. Available: http://www.asctec.de.

[18] J. Andersh, B. Mettler, and N. Papanikolopoulos, Experimental investigation of teleoperation performance for miniature rotorcraft, *In Proc. Decision and Control, jointly with 28th Chinese Control Conference*, pp. 6005-6010, Dec. 15-18, Shanghai, China, 2009.

[19] R. Carloni, V. Lippiello, M. DAuria, M. Fumagalli, A. Mersha, S. Stramigioli, and B. Siciliano, Robot vision: Obstacle-avoidance techniques for unmanned aerial vehicles,*Robotics Automation Magazine, IEEE*, vol. 20, pp. 22-31, 2013.

[20] P. Stegagno, M. Basile, H. Bulthoff, and A. Franchi, A semi-autonomous uav platform for indoor remote operation with visual and haptic feedback, *In Proc. IEEE Conference on Robotics and Automation (ICRA)*, pp. 3862-3869, May 2014.

[21] P. Stegagno, M. Basile, H. H. Blthoff, and A. Franchi, Vision-based autonomous control of a quadrotor uav using an onboard rgb-d camera and its application to haptic teleoperation, *2nd IFAC Work. on Research, Education and Development of Unmanned Aerial Systems*, Compiegne, France, 2013.

[22] A. Ruesch, A. Mersha, S. Stramigioli, and R. Carloni, Kinetic scrolling-based position mapping for haptic teleoperation of unmanned aerial vehicles, *In Proc. IEEE Conference on Robotics and Automation (ICRA)*, pp. 3116-3121, May 2012.

[23] A. Mersha, S. Stramigioli, and R. Carloni, On bilateral teleoperation of aerial robots, *IEEE Transactions on Robotics*, vol. 30, pp. 258-274, Feb 2014.

[24] A. Mersha, S. Stramigioli, and R. Carloni, Switching-based mapping and control for haptic teleoperation of aerial robots,*In Proc. IEEE Conference on Intelligent Robots and Systems (IROS)*, pp. 2629-2634, 2012.